Chemical Kinetics in Porous Walled Reactors: The Decomposition of Hydrogen Peroxide Vapor

CHARLES N. SATTERFIELD, ROBERT C. REID, and ALFRED E. WECHSLER

Massachusetts Institute of Technology, Cambridge, Massachusetts

This study explored the reaction characteristics of a novel type of reactor consisting of a tube whose walls are made of a finely porous material through which an inert gas or a reactant in stoichiometric excess can be passed to reduce diffusion of the reacting species to the vessel surface. It was thought that such a reactor might provide a new method of ascertaining the relative contributions of homogeneous and surface effects in a gaseous reaction involving both, or a method of minimizing surface effects in chemical synthesis.

Although simultaneous diffusion and chemical reaction within porous catalyst particles has been studied extensively, both theoretically and experimentally, very little has been published about carrying out a chemical reaction in a flow reactor with porous walls. Hartnett and Eckert (7) discuss theoretical considerations involved in the combustion of a fluid coolant after passage through a porous wall, and Weger and Effron (22) investigated the cooling of aerodynamic surfaces by endothermic reactions on a porous tube impregnated with a catalyst.

This study examined the effects of inert-gas injection through a porous tube on the rate of heterogeneous decomposition of hydrogen peroxide vapor present in the gas flowing axially through the tube. This reaction was chosen as the model system because it is relatively simple, because homogeneous reaction is negligible under the conditions chosen, because only one set of products is formed, and because it is a reaction with which the authors have had considerable experience. However the method of mathematical analysis is a general one for a first-order reaction in which change in number of moles causes insignificant effects.

APPARATUS AND PROCEDURE

Porous-walled tubes of ultra-fine porosity Pyrex 7740 glass (*10*) and type-316 stainless steel [designated as 5μ particle removal size, type H (*4*)] were jacketed, respectively, with nonporous Pyrex and stainless steel tubes, wrapped with heating wires, thermally and electrically insulated, and mounted vertically. Figure 1 shows a schematic diagram of the porous stainless steel reactor. The Pyrex reactor was similar in construction. In both reactors an inert gas could be forced into the jacket and through the porous wall. Pertinent dimensions of both reactors are tabulated in Table 1. Mainstream gas from high-pressure cylinders was throttled, regulated, and then bubbled through concentrated liquid hydrogen peroxide, thus producing a vapor containing up to 4 mole % hydrogen peroxide, several per cent water, and the remainder inert carrier gas. Variation in the concentration of hydrogen peroxide vapor was effected by changing the temperature of the bath in which the bubblers were immersed. The hydrogen peroxide content of the mainstream gas before and after the reactor was determined by bubbling a measured quantity of gas through water and titrating the resultant solution with standardized potassium permanganate.

Gas flow rates were measured with calibrated capillary flowmeters. Temperatures and pressures within the reactor were measured at various locations with iron-constantan thermocouples and a precision potentiometer, and manometers filled with water or mercury. A schematic diagram of the experimental apparatus is shown in in Figure 2.

Experimental runs consisted of measuring inlet and outlet concentrations of hydrogen peroxide vapor under the following ranges of operating conditions: mainstream flow rates from 0.04 to 0.40 g. moles/min.; injectant flow rates from 0 to 0.40 g. moles/min.; reactor temperatures from 85° to 178°C.; hydrogen peroxide partial pressures from 0 to 0.04 atm.; carrier gas of nitrogen, carbon dioxide, helium, Freon 12 (CCl_2F_2), or Freon 114 ($C_2Cl_2F_4$); and injectant gas of nitrogen, carbon dioxide, helium, or Freon 12.

CHARACTERISTICS OF POROUS MATERIALS

Table 2 shows the porosity characteristics and other properties of the porous materials. The average pore radii as calculated from the ratio $2V_g/S_g$ agree closely with the values as determined by the mercury injection porosimeter. Pore size distributions (*21*) were determined by the mercury porosimeter method. For the stainless steel 80% of the pore volume was represented by pores of average radius between 4 and 10μ. For the Pyrex, 80% of the pore volume was represented by pores between 0.7 and 2-μ radius. These pores are sufficiently large that diffusion occurs essentially by ordinary bulk diffusion. Only for a few runs with hydrogen peroxide and helium was it necessary to make a slight correction for Knudsen diffusion. Diffusion in a porous structure may be expressed in terms of an effective diffusivity, $D_{eff} = \frac{D\theta}{\tau}$. D_{eff} then refers to flux based on total cross section of porous solid normal to direction of diffusion. The porous structure was assumed here to follow the mathematical model of Wheeler (*24, 25*) in which the pores are visualized as cylinders of uniform radius intersecting any plane at an average angle of 45 deg. Hence $\tau = 2$. Values of D for the various mixtures in bulk diffusion were calculated by the methods of Hirschfelder, Curtiss, and Bird (*8*). Results are expressed in terms of D or D_{eff} as defined above.

HYDROGEN PEROXIDE DECOMPOSITION

Even at relatively low temperatures and on almost all surfaces hydrogen peroxide vapor decomposes to water and oxygen at readily measurable rates. The low-temperature decomposition is reported to occur heterogeneously by approximately a first-order reaction on Pyrex (*1, 9, 15*) and on stainless steel (*15, 26*). The rates of heterogeneous reaction, particularly initially, are strongly dependent upon the previous surface treatment and may also be affected by the length of time during which the surface has been exposed to hydrogen peroxide (*15*).

The published rate data on nonporous surfaces treated in the most closely comparable way to those in the present studies are those of Stein (*15*) on acid washed, fused Pyrex, and Hoare, Protheroe, and Walsh (*9*) on Pyrex cleaned in 40% hydrogen flouride. For stainless steel Stein reported some values on pickled and passivated surfaces, but these are much more active than untreated surfaces which have been exposed only to hydrogen peroxide. Data on untreated 304 surfaces were recently reported by Yeung (*26*). Little effect of inert gases such as air, carbon dioxide, oxygen and water vapor on the heterogeneous decomposition of hydrogen peroxide was

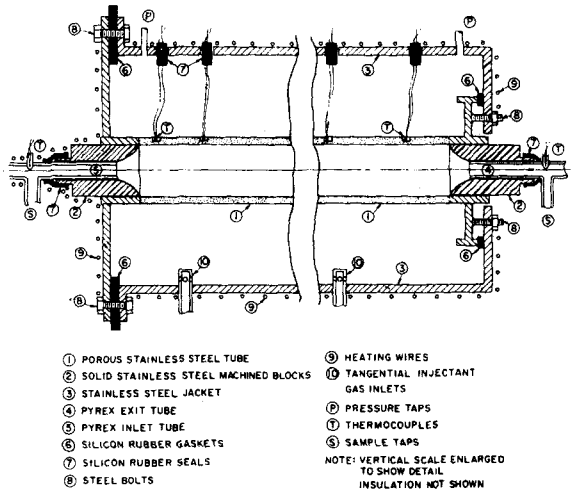

Fig. 1. Diagram of porous stainless steel reactor.

noted by Baker and Ouellet (*1*) and Yeung (*26*), although Forst and Giguere (*6*) mention that inert gases tend to inhibit the heterogeneous reaction at low pressures.

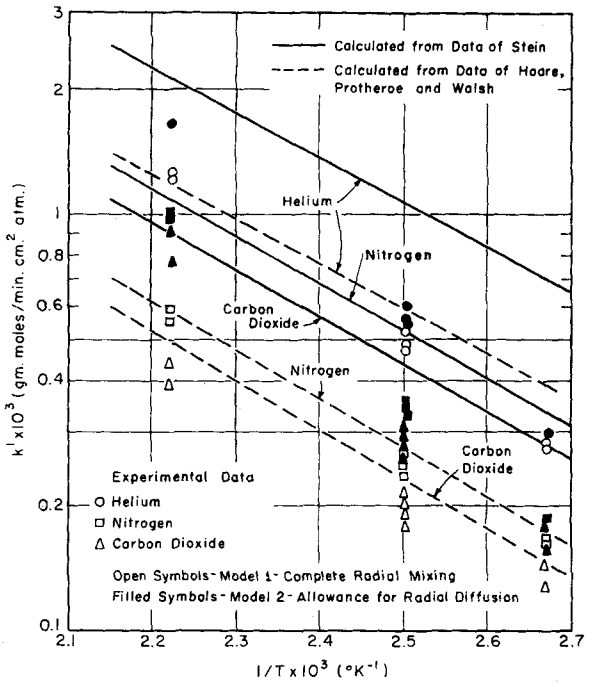

Fig. 3. Effect of temperature upon apparent rate constants (porous Pyrex reactor).

THEORY

Reaction in a Porous-Walled Tube Without Injection Through the Wall

To provide a basis for comparison of results with injection through the wall the case of no injection was first studied. Two simplified limiting models were considered for mathematical analysis. (In the remainder of this discussion hydrogen peroxide is considered as the active component and the reaction is assumed to be first-order. The change in number of moles on reaction has a negligible effect here since the hydrogen peroxide is dilute. The analysis applies to any first-order heterogeneous reaction of this type.)

Model 1: The flow of hydrogen peroxide and the carrier gas is well mixed radially but not axially (plug flow).

Model 2: The gas flows through the reactor with a flat velocity profile and mass transfer occurs radially by molecular diffusion only.

In both models the hydrogen peroxide decomposes as it diffuses through the porous wall. The exact behavior of the actual reactor will depend upon the Reynolds number, entrance and exit effects, density differences, and other factors, but can be approximated by these limiting models.

The extent of reaction as measured by the decrease in the partial pressure of hydrogen peroxide as the reacting gas flows along the porous-walled reactor can be expressed in terms of an apparent rate constant based on the projected inside tube area. For model 1 and an isothermal system this is

$$\ln \frac{P_{in}}{P_{out}} = \frac{2\pi R_1 Z_p (rf) P_T k'}{G_{ms,t}} \quad (1)$$

For materials of relatively low activity such as Pyrex and stainless steel, in which the reactant penetrates the porous structure deeply, the rate constant thus calculated will greatly exceed the true intrinsic rate constant based on the actual area, that is $k' >> k$. The rate of decomposition per unit projected area of the porous wall is given by $k'P_1$ or $-D_{eff}\left(\frac{dP}{dR}\right)_{R=R_1}$ and is related to the characteristic parameters of the porous material, the diffusivity of hydrogen peroxide, and the true (intrinsic) heterogeneous reaction rate constant k by the following expression (*21*):

$$k'P_1 = -D_{eff}\left(\frac{dP}{dR}\right)_{R=R_1} = \frac{P_1 D\theta h}{2}\left[\frac{K_1(hR_1)}{K_0(hR_1)}\right] \quad (2)$$

where h is a modulus similar to that of Thiele (*20*) defined as

$$h = \sqrt{\frac{4k}{\bar{r}D}} = \sqrt{\frac{S_g \rho_P k}{D_{eff}}} \quad (3)$$

For diffusion into cylindrical walls of the radii studied here values of k' as calculated from Equation (2) do not differ greatly from those calculated for diffusion into a semi-infinite flat plate. Mathematical relationships for the latter geometry have been previously published (*20, 24, 25*). Values of k' can be computed from Equations (2) and (3) with values of the true heterogeneous rate constant and compared with values of k' obtained from experimental data and from Equation (1).

For model 2, where there is diffusion resistance within the mainstream,

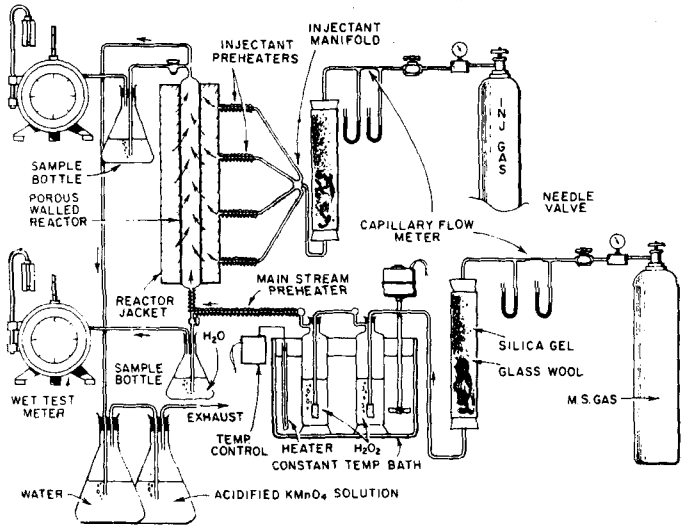

Fig. 2. Schematic diagram of apparatus.

Table 1. Characteristics and Dimensions of Reactors

	Porous Pyrex reactor	Porous stainless steel reactor
Reactor dimensions, inside diameter	3.38 cm.	3.40 cm.
Wall thickness	0.44 cm.	0.20 cm.
Length of porous wall	69.4 cm.	77.0 cm.
Superficial area of porous material in reactor	738.0 sq. cm.	835.0 sq. cm.
Area of nonporous material in reactor	154.0 sq. cm.	28.0 sq. cm.
Inside diameter of jacket	9.5 cm.	10.2 cm.
Inlet and outlet tube dimensions		
Inside diameter	1.2 cm.	0.91 cm.
Outside diameter	1.4 cm.	1.13 cm.

the basic equations governing the amount of reaction on the surface of a cylindrical reactor have been derived by Damkohler (5), Mickley, Sherwood, and Reed (12), and Baron, Manning, and Johnstone (2). For a first-order surface reaction Baron et al. present an equation which in the present nomenclature and units becomes

$$\frac{P_{out}}{P_{in}} = \sum_{n=1}^{\infty} \frac{4}{\eta_n^2 \left[1 + \eta_n^2 \left(\frac{D}{k' R_1}\right)^2\right]} e^{-\eta_n^2 D \pi P_T Z_p / G_{ms,t}} \quad (4)$$

where

$$\frac{k' R_1}{D} = \eta_n \frac{J_1(\eta_n)}{J_0(\eta_n)} \quad (5)$$

As with model 1 values of k' calculated from experimental data and Equations (4) and (5) may be compared with values computed from Equations (2) and (3).

Reaction in a Porous-walled Tube with Injection Through the Wall

Injection of inert gas through the porous wall can be considered to have two major effects: sweeping of the pores to reduce diffusion of hydrogen peroxide molecules into the pores, and formation of a boundary layer of inert gas which retards diffusion of the hydrogen peroxide to the wall. The first effect can be analyzed by a modification of the models used above. It was expected that the importance of the second effect could be estimated by examination of the agreement between the experimental results and the results predictable from a model which takes pore sweeping into account.

The assumption of plug flow (model 1) was made for simplicity and because no-injection results indicate that plug flow appears to be approached in the system used. As a further mathematical simplification a flat-plate system was used for computation of the effects of injection rather than the cylindrical system used previously. The difference between the results predicted by flat-plate and cylindrical models is small for the case of no injection, and there is no reason to suggest that a greater difference will occur in models which take injection into account. If one considers forced flow of injectant through the pores in opposition to the normal direction of diffusion of hydrogen peroxide, the ratio of the apparent rate constant with injection to the apparent rate constant in the absence of injection (k'_I/k'_{NI}) is

$$k'_I/k'_{NI} = -w + \sqrt{w^2 + 1} \quad (6)$$

where

$$w = \frac{G_{i,y}\sqrt{r}}{P_T \sqrt{4kD}} \quad (7)$$

The term $G_{i,y}$ is the flow rate of injectant per unit area within any pore in a direction perpendicular to the direction of mainstream flow and is calculated by assuming perfect distribution over the total wall area; that is one finds

$$G_{i,y} = G_{i,t}/2\pi R_1 Z_p \theta \quad (8)$$

When the effect of dilution of the mainstream gas by the injectant gas is taken into account, Equation (1) becomes

$$k'_I = \left[\frac{\ln P_{in}/P_{out}}{\ln \frac{G_{i,t} + G_{ms,t}}{G_{ms,t}}} - 1\right] \frac{G_{i,t}}{2\pi R_1 Z_p P_T} \quad (9)$$

Experimental values of the ratio k'_I/k'_{NI} obtained from Equations (1) and (9) can be compared with the theoretical results predicted by Equations (6) and (7).

RESULTS AND DISCUSSION

Reaction Without Injection—Porous Pyrex Reactor

Figure 3 shows the calculated and experimental values of the apparent rate constants for the porous Pyrex reactor as a function of temperature for various carrier gases. Examination of the figure shows good general agreement between the present experimental rate data and those calculated from previously reported data, although better agreement is obtained with Hoare's values than with Stein's data. There are two possible explanations. Stein (17) showed that there was considerable variation in the rate constant observed for reaction on similar glasses which had been given different surface treatments and even found a substantial variation in glasses which had been treated identically. Thus the better agreement with the data of Hoare may have resulted from a fortuitous choice of a particular sample of Pyrex glass. Secondly the calculated values of the apparent rate constant are based on the assumption that there is no effect of the type of carrier gas on the true rate constant; that is the effect of the inert gas on the calculated apparent rate constant appears only in the diffusion coefficient for the hydrogen peroxide gas mixture. In Stein's work hydrogen peroxide vapor was prepared by boiling aqueous solutions of liquid hydrogen peroxide;

Table 2. Characteristics of Porous Materials

Parameter	Method of measurement	Porous Pyrex	Porous stainless steel
Porosity, θ	Density measurements	0.36	0.38
Pore volume, V_g	Mercury injection porosimeter	0.26 cc./g.	0.075 cc./g.
Density of porous material, ρ_P	Mercury displacement	1.38 g./cc.	5.07 g./cc.
Density of solid material, ρ_t	Mercury displacement	2.23 g./cc.	7.97 g./cc.
Specific surface area, S_g	B.E.T. method	0.36×10^4 sq. cm./g.	0.018×10^4 sq. cm./g.
Average pore radius r	Mercury injection porosimeter	1.30×10^{-4} cm.	7.0×10^{-4} cm.
$2V_g/S_g$	From measurements above	1.44×10^{-4} cm.	8.3×10^{-4} cm.

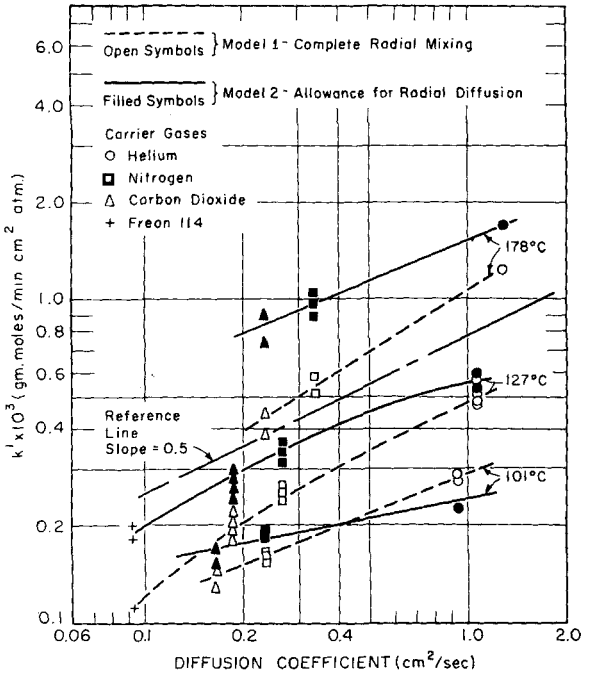

Fig. 4. Variation of apparent rate constant with diffusion coefficient (porous Pyrex reactor).

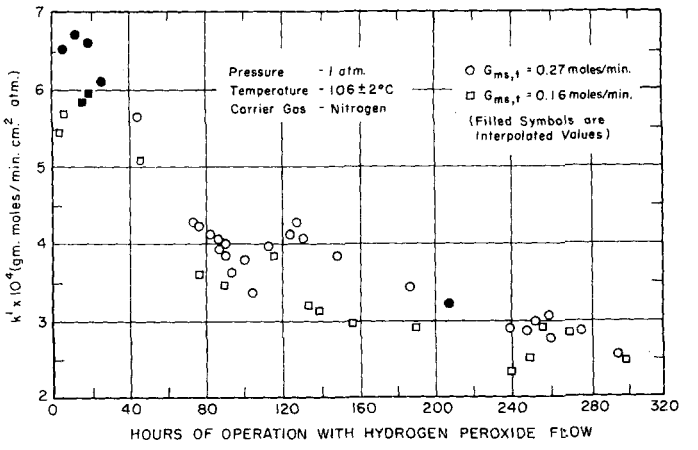

Fig. 5. Effect of contact time upon apparent rate constant. Porous stainless steel reactor.

therefore water was the carrier gas and was present in high concentrations. In the present work and in that of Hoare et al. nitrogen or other carrier gases were used, and the gas mixtures contained only small amounts of water. If water or the other carrier gases did have an effect on the true rate constant, it would be expected that the present data would compare more closely with those of Hoare rather than with those of Stein. Figure 3 shows that the activation energies as calculated from the complete radial mixing model are in excellent agreement with the values reported by both previous investigators.

In theory the apparent rate constant k' should be proportional to the square root of the diffusion coefficient. Figure 4 shows good agreement between theory and the results for model 1. This agreement and the values of the activation energy suggest that the flow in the reactor may have been approximated by well mixed or plug flow, even though the Reynold's number of the mainstream flow was below 2,000, and in the region normally ascribed to laminar flow. The mixing and turbulence is probably caused primarily by the effects of the entrance and exit zones which contained constrictions, and possibly by wall roughness.

Other experimental observations indicated little effect of flow rate on the apparent rate constant and no aging effect of the reactor surface.

Reaction Without Injection—Porous Stainless Steel Reactor

In the porous stainless steel reactor an aging effect as shown on Figure 5 made interpretation of the results difficult. The decrease in the rate constant may have several possible explanations. *Passivation of the surface*—This phenomenon is known to occur in actual plant operation in stainless steel pipes which carry hydrogen peroxide vapor. *Reaction and/or removal of impurities*—Impurities of unknown origin could have decomposed or reacted during the operation; since most impurities have a higher catalytic activity for hydrogen peroxide than stainless steel, a decrease in the reaction rate could be expected. *Physical change of the stainless steel*—A phase transformation of the stainless steel due to heating and cooling may have resulted in a form of stainless steel which was less catalytic to hydrogen peroxide than the original form. Such phase transformations have been reported to take place during 100 to 1,000 hr. of heating (*3, 16*).

After the activity had become reduced to a reasonably steady state level, runs were made in which the effects of temperature and carrier gas on the apparent rate constant could be determined. The data are shown in Figure 6 together with curves calculated from intrinsic rate constants measured by Yeung (*26*). The discrepancy may be due at least in part to the fact that Yeung's reactor was type-304 stainless steel, whereas the porous stainless steel reactor here was type-316. The porous stainless steel reactor, which had relatively smooth inlet and outlet nozzles, also exhibited a greater effect of flow rate on the apparent rate constant than was shown in the porous Pyrex reactor.

The two principal sources of error in comparing theory and experiment, as in Figures 3 and 6, are the extent to which the true effective diffusivity in the porous structure can be represented by the simplified mathematical model (see later), and variation in intrinsic surface rates from sample to sample and that caused by different treatments. When one considers the possible variability of surface activities, the extent of agreement between present experimental results on both kinds of surfaces and those predicted from rate constants previously reported for smooth surfaces is surprisingly good and indicates the applicability of the models of the porous structure and of the reactor.

Reaction With Injection—Porous Pyrex Reactor

The results of experiments in which inert gases were injected through the reactor walls are shown in Figure 7, where the ratio of the apparent rate constants with and without injection are plotted vs. w, a parameter which combines the injection, reaction, and diffusion parameters and is a measure of the theoretical effectiveness of the sweep gas. Since the model allows for pore sweeping but not for radial bulk diffusion, one might expect the experimental results to lie below the model curve; the difference between the model curve and the experimental data would then be a measure of the effect of boundary-layer formation. However a substantial part of the results in fact lie above the model curve. A discussion of the degree to which the model actually represents the physical situation will aid in analyzing this discrepancy.

Uniformity of Injection. Uniformity of injection of inert gases over the sur-

face of the reactor was assumed in the derivation of the model equations. Measurements indicated that no gross permeability discontinuities were present in either reactor. In the porous Pyrex reactor the high ratio of the pressure differential across the porous wall to the axial pressure decrease of the mainstream gas on flowing through the reactor assured uniform injection. In the porous stainless steel reactor however the greater inherent permeability led to a smaller pressure drop across the wall, and there may have been undesirable recirculation flow during experiments at high flow rates.

Accuracy of the Model Parameter Values. Equations (7) and (8) may be combined to give

$$w = \left[\frac{G_{i,1}}{4\pi R_1 Z_p P_T}\right]\left[\frac{\sqrt{\bar{r}}}{\theta\sqrt{4kD}}\right] \tag{10}$$

The first term consists of measured quantities and is believed accurate to ±5%. The second term however consists of estimated and calculated quantities and may be subject to considerable error. The values of the porosity and D are known to within 10%. The value of the average pore radius may be in considerably greater error. Incidentally, previous investigators and manufacturers report a variety of average pore radii for these materials (*4, 10, 13, 18*). The tortuosity factor was taken here to be 2, in accordance with the Wheeler model, but the true value could be substantially different. The values of the rate constant were obtained from the data for experiments without injection. Values of k as a function of temperature may be calculated with model 1 or model 2. The value of k used in Equation (10) was arbitrarily chosen as the average of the values calculated from model 1 and model 2 for similar conditions of temperature, flow, and carrier gas. These average values could have been in error by a factor of as much as 2, resulting in a corresponding error in w.

Pore Size Distribution. The characterization of irregularly shaped, continuous, and discontinuous pores by open cylinders of identical radius is a highly simplified description of the porous materials. Pore size distributions were measured and the effects of pore size variation were estimated by including the distribution in the derivation of the model equations. This results in a modification of Equation (6) to give

$$\frac{k'_I}{k'_{NI}} = \frac{\int_0^\infty n(r)r^2\left[\frac{\Psi r^2}{DP_T} + \sqrt{\left[\frac{\Psi r^2}{DP_T}\right]^2 + \frac{4k}{rD}}\right]dr}{\int_0^\infty n(r)r^2\sqrt{\frac{4k}{rD}}\,dr} \tag{11}$$

The integration indicated above was carried out graphically for several particular operating conditions and showed that values of k'_I/k'_{NI} calculated with the pore size distribution function could be 10 to 20% higher than the corresponding values of k'_I/k'_{NI} calculated with the assumption of uniform pore size. This effect can be explained qualitatively on the basis that the larger pores carry most of the injectant flow and that the flow in the smaller pores is correspondingly less effective in reducing diffusion into the pores. Since a large portion of the area upon which reaction occurs is in the small pores, the reduction in the apparent rate constant due to injection will not be as great when a substantial pore size distribution exists as when the pores are essentially uniform in size.

Wall Roughness and Nonporous Area. Joining and end sections of the reactors were constructed of nonporous materials. These discontinuities and those produced by sample taps decreased the uniformity of injection and tended to increase turbulence and mixing within the reactor.

Boundary-Layer Formation. Several additional factors could have limited the formation of boundary layers and thereby reduced the blanketing effect of the inert gas. For the experimental conditions of laminar flow through the porous wall the velocity of injectant in the pores varies with the square of the pore radius. Therefore the distribution of pore radii results in jets of varying velocities emerging from the wall. The injection velocity was relatively large compared with that normally encountered in the analysis of flow in ducts with coolant injection (*11*), and increased mixing and turbulence could have resulted. When different carrier gases were used as the injectant and mainstream, the density differences facilitated mixing.

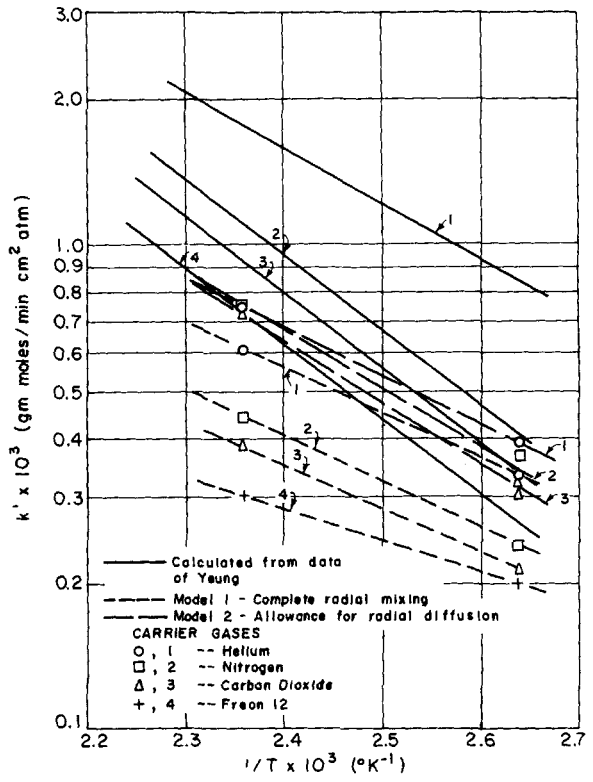

Fig. 6. Apparent rate constants in porous stainless steel reactor.

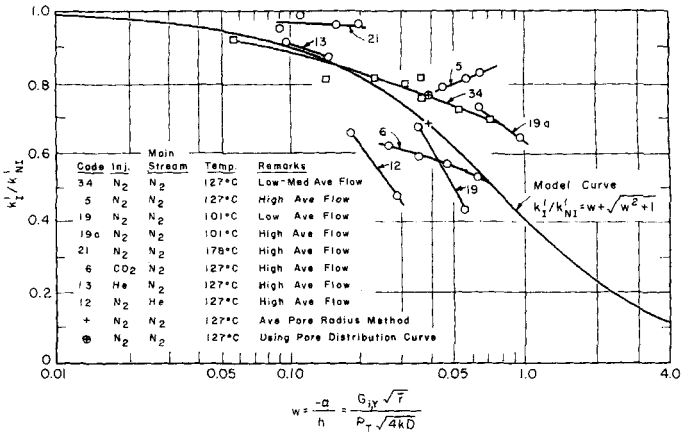

Fig. 7. Effect of injection parameter w upon ratio of apparent rate constants with and without injection. Porous Pyrex reactor.

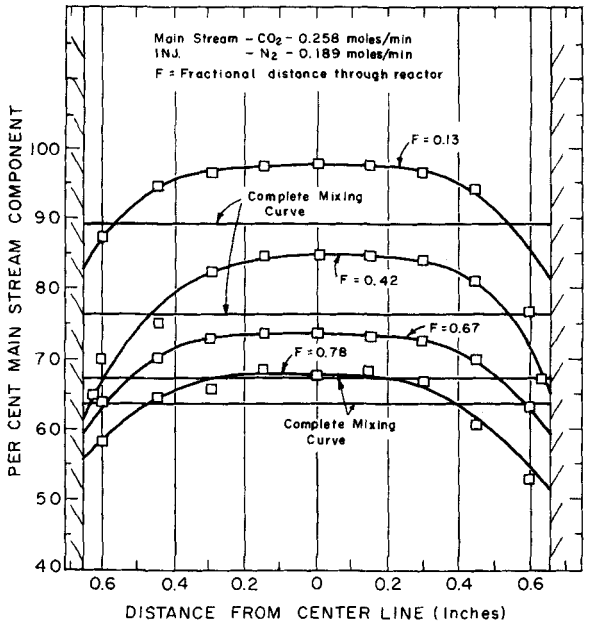

Fig. 8. Radial concentration profiles at certain axial distances in porous Pyrex reactor. Nonreacting system at 25°C.

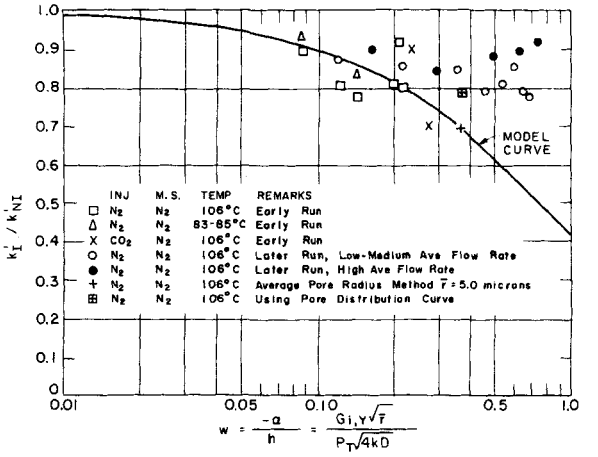

Fig. 9. Effect of injection parameter w upon ratio of apparent rate constants with and without injection. Porous stainless steel reactor.

The effect of the constrictions at the inlet and outlet of the reactors has already been mentioned. Because of these factors boundary-layer formation may not have been as significant as desired.

Several experiments were carried out in a nonreactive, room temperature system wherein concentration profiles were measured within the porous Pyrex reactor during conditions of injection. For conditions of vertical flow of nitrogen as the mainstream gas with carbon dioxide as the injectant, concentration profiles are shown in Figure 8 for several downstream distances. The straight lines indicate the average concentration if the injectant and mainstream gas were completely mixed. Points near the wall were taken with 0.010 in. diameter steel probes resting on the wall (*14*). It is seen that the boundary-layer effect is not very large.

Experimental Errors. The experimental values of the apparent rate constants with and without injection are the integrated values throughout the entire reactor, and the inaccuracies inherent in the evaluation of integrated reaction rate data are well known. There was usually a substantial dilution of the mainstream gas by the injectant which increased the variation of the partial pressure of hydrogen peroxide in the gas stream. The estimated error in the experimentally measured values of the ratio of apparent rate constants is about 10%.

Isothermal Operation. The above analyses assume that the temperature is uniform throughout the porous structure. There have been a number of papers published recently which have presented methods of estimating temperature gradients in porous catalyst particles and indicated the effects that would be expected by neglecting possible temperature gradients. See for example Tinkler and Metzner (*19*) and Weisz and Hicks (*23*). In the authors' studies with the stainless steel reactor, thermocouples embedded in the porous wall showed no significant temperature increase over that recorded by the thermocouples measuring inlet and exit main gas temperatures. This is consistent with the good thermal conductivity of a metal. Similar measurements were not possible in the porous Pyrex reactor. However it was estimated that the maximum temperature gradient through the porous glass would not exceed 10°F. under the most extreme conditions studied here, namely the diffusion of hydrogen peroxide through helium, no use of injectant gas, and a partial pressure of hydrogen peroxide in bulk stream of 0.04 atm. When one also considers the low activation energy of the hydrogen peroxide decomposition reaction, little error is introduced by the assumption of isothermal wall conditions.

Comparison of Experimental Data and Model

The reasons given above explain why the experimental data do not agree closely with the model. With the tortuosity factor of 2, if it were assumed that the correct value of $\bar{r}/k$ is about one-third of the value accepted in the calculations leading to the positioning of the data points in Figure 7 [an adjustment of this magnitude is substantiated in the above discussion and the direction of the adjustment is such as to bring the modified values of the pore radius and the rate constant into more close agreement with those previously found (*9, 15, 26*)], then the abscissa of each experimental point of Figure 7 is displaced to the left by a constant value. Such an adjustment would cause the data to lie below the model curves and furnish a logical explanation for the trends and discrepancies observed.

The degree to which injection reduces the apparent rate constant is greater during low-temperature operation (line 19) than during high-temperature operation (lines 21 and 34). Similarly injection has a greater effect on the reduction of the apparent rate constant in experiments with low average flow rates than with high average flow rates. Lower flow rates and reactor temperatures are more conducive to boundary-layer formation owing to the less intense turbulence. Injection of high molecular weight gases into a low molecular weight mainstream gas is more effective in reducing the apparent rate constant due to favorable boundary-layer formation at the wall; conversely, injection of a low molecular weight gas into heavier mainstream gases is less effective in reducing the apparent rate constant. These effects are confirmed by experiments in nonreactive systems.

The degree to which experimental data points lie below the model curve is an estimate of the ratio of the actual partial pressure of hydrogen peroxide at the wall to that at the wall in a radially completely mixed system. For example if one assumed that the correct value of $\bar{r}/k$ were one-third that used in Figure 7, in experiments where carbon dioxide was injected into a main stream of nitrogen, the ratio $P_{H_2O_2,\ wall,\ actual}/P_{H_2O_2,\ wall,\ mixed}$ would vary from 0.72 to 0.76. In the concentration profiles determined in the absence of reaction (Figure 8) the cor-

responding ratio varied from 0.75 to 0.92 for the same average flow rates but for slightly lower rates of injection. This agreement suggests that the lower value of $\bar{r}/k$ is a more realistic characterization of the porous substances.

At very high rates of injection boundary-layer formation was probably reduced owing to back mixing, turbulence, and recirculation. Examination of the model curves shows that in order to decrease the apparent rate constant to a value of one-tenth the value obtained with no injection, very high injection rates would be needed. These rates could probably not be achieved in the present apparatus because of structural limitations. Also the accompanying high degree of dilution is undesirable.

Reaction With Injection—Porous Stainless Steel Reactor

Experimental results and a model curve for conditions of injection through the wall of the porous stainless steel reactor are shown in Figure 9. The discussion above concerning the applicability of the model to the physical situation applies equally well to the porous stainless steel reactor. The experimental results follow the same trends as in the porous Pyrex reactor; however there is less reduction of the apparent rate constant. If modified values of $\bar{r}/k$ are accepted, the experimental data points will also lie below the model curve. The stainless steel reactor had a somewhat greater pore size distribution, and the possibility of back mixing and recirculation also add to the discrepancy between the model and the experimental results.

A comparison of the data in the porous stainless steel reactor with the heat transfer data of Stubbs (*17*) can be made. Stubbs used a 1 in. I.D. porous stainless steel tube in which heat was transferred from the wall to the stream gas flowing through the tube. The heat transfer coefficient decreased rapidly at first when the injection velocity was increased, but the decrease soon approached a constant value (contrary to theory) so that a maximum of 20% reduction in the heat transfer coefficient could be obtained at high injection rates. Although the systems are quite different in their characteristics and in the measured quantities, the results indicate comparable effects of injection and comparable deviation from theory.

CONCLUSIONS

The magnitude and the dependence on temperature and type of gas of the apparent rate constant in a porous walled reactor in the absence of injection was adequately predicted in terms of models which employ the characteristic parameters of porous materials and rates of reaction on nonporous materials. The injection of gas through the wall of a porous reactor significantly reduces the apparent rate constant; the greatest reductions occur when low reactor temperatures and high molecular weight injectant gases are used. However with the rates of injection which would not be detrimental to the study of the mechanism of a reaction or to use in chemical synthesis the overall reaction rate is still much higher than in a nonporous reactor of a similar material, so this does not appear to be a practical means of avoiding heterogeneous reaction.

The operating characteristics of porous-walled reactors may suggest possible applications to other chemical reactions. For example the walls of a porous reactor may be impregnated with a catalyst and one reactant forced through the wall by means of a pressure gradient, thus minimizing counterdiffusion of gases into and out of the catalyst structure and providing ease of control of residence times and of flow. Porous-walled reactors also provide a method of feeding one component into the main reactant stream at a uniform rate to achieve a uniform concentration axially. They may also provide a method of achieving more uniform temperatures axially than can be obtained in the usual multitube packed catalyst reactor.

ACKNOWLEDGMENT

The authors wish to acknowledge the financial support of the National Science Foundation under Grant G6306 and that of the Office of Naval Research under contract Nonr 1841(11). The pore size distribution measurements were made through the courtesy of Dr. C. R. Nelson of the Shell Development Company.

NOTATION

D = molar diffusivity of hydrogen peroxide in carrier gas, (mole/min.cm.atm.), $D_{eff} = D\theta/\tau$, and is based on total cross section of porous solid

G = mainstream flow rate, (mole/min.)

$G_{i,t}$ = total injectant flow rate, (mole/min.)

$G_{i,y}$ = injectant flow rate per unit area within pore, in y direction, (mole/min. sq.cm.)

$G_{ms,t}$ = mainstream flow rate at reactor inlet, (mole/min.)

h = modulus defined by Equation (3)

J_0, J_1 = Bessel function, first kind, zero and first order

k = true (intrinsic) first-order rate constant, (mole/min. sq.cm. atm.)

k', k'_{NI} = apparent rate constant without injection, based on projected area of porous wall, (mole/min. sq.cm. atm.)

k'_I = apparent rate constant with injection, based on projected area of porous wall, (mole/min. sq.cm. atm.)

K_0, K_1 = modified Bessel functions, second kind, zero and first order

$n(r)$ = number distribution function for pore radius, cm.$^{-1}$

P = partial pressure of hydrogen peroxide, atm.

P_1 = partial pressure of hydrogen peroxide at inside reactor wall, atm.

P_{in} = partial pressure of hydrogen peroxide at reactor inlet, atm.

P_{out} = partial pressure of hydrogen peroxide at reactor outlet, atm.

P_T = total pressure in reactor, atm.

$\bar{r}$ = average pore radius, cm.

r = pore radius, variable, cm.

rf = roughness factor

R = radial coordinate of reactor models

R_1 = inner radius of reactor wall, cm.

R_2 = outer radius of reactor wall, cm.

S_g = specific surface area of porous material, (sq.cm./g.)

T = temperature, (°C.) or (°K.)

V_g = pore volume of porous material, (cc./g.)

Y = coordinate perpendicular to flow direction for models with flat-plate system

Z_p = length of porous section of reactor, cm.

Greek Letters

α = parameter equal to $G_{i,Y}/DP_T$, cm.$^{-1}$

α_n = nth root of Bessel equation $J_0(x) = 0$

η_n = root of equation $\eta_n J_1(\eta_n)/J_0(\eta_n) = k'R_1/D$

θ = volume void fraction or porosity

ρ_p = density of porous material (g./cc.)

τ = tortuosity factor, taken here to equal 2

Ψ = flow coefficient per pore, (mole/min. cm.^{4})

LITERATURE CITED

1. Baker, B. E., and C. Ouellet, *Can. J. Research*, **B23**, 167 (1945).
2. Baron, Thomas, W. R. Manning, and H. F. Johnstone, *Chem. Eng. Progr.*, 48, 125 (1952).
3. British Iron and Steel Research Assoc., "Atlas of Isothermal Transformation

Diagrams of B. S. En Steels," 1 ed., Iron and Steel Institute, London, England (1949).
4. Campbell, J. B., *Materials and Methods*, **42**, 98 (April, 1955).
5. Damkohler, G., *Z. Electrochem.*, **42**, 846 (1936).
6. Forst, W., and P. A. Giguere, *J. Phys. Chem.*, **62**, 340 (1958).
7. Hartnett, J. P., and E. R. G. Eckert, "Heat Transfer and Fluid Mechanics Institute," Berkeley, California, Preprints, p. 54 (1958).
8. Hirschfelder, J. O., C. F. Curtiss, and R. B. Bird, "Molecular Theory of Gases and Liquids," Wiley, New York (1954).
9. Hoare, D. E., J. B. Protheroe, and A. D. Walsh, *Nature*, **182**, 654 (1958).
10. Lillie, H. R., Personal communication, Corning Glass Works, Corning, New York (November 2, 1959).
11. Mickley, H. S., R. C. Ross, A. L. Squyers, and W. E. Stewart, *Natl. Advisory Comm. Aeronaut., Tech. Note No.* 3208 (1954).
12. Mickley, H. S., T. K. Sherwood, and C. E. Reed, "Applied Mathematics in Chemical Engineering," 2 ed., p. 298, McGraw-Hill, New York (1957).
13. Ritter, H. L., and L. C. Drake, *Ind. Eng. Chem. Anal. Ed.*, **17**, 782 (1945).
14. Sane, J. O., S.M. thesis, Mass. Inst. Technol., Cambridge, Massachusetts (1959).
15. Satterfield, C. N., and T. W. Stein, *Ind. Eng. Chem.*, **49**, 1173 (1957).
16. Schvartz, G. L., and M. M. Krisstal, "Corrosion of Chemical Apparatus," p. 82, translated from the Russian, Chapman and Hall, Ltd., London, England (1959).
17. Stubbs, H. E., Sc.D. thesis, Univ. Mich., Ann Arbor, Michigan (1959).
18. Tammaro, N. J., Personal communication, Corning Glass Works, Corning, New York (December 8, 1958).
19. Tinkler, J. D., and A. B. Metzner, *Ind. Eng. Chem.*, **53**, 663 (1961).
20. Thiele, E. W., *ibid.*, **31**, 916 (1939).
21. Wechsler, A. E., Sc.D. thesis, Mass. Inst. Technol., Cambridge, Massachusetts (January, 1961).
22. Weger, E., and E. Effron, Paper presented at Annual Christmas Symposium of Industrial and Engineering Chemistry Division of American Chemical Society at Johns Hopkins Univ., Baltimore, Maryland (December 28, 1959).
23. Weisz, P. B., and J. S. Hicks, *Chem. Eng. Sci.*, **17**, 265 (1962).
24. Wheeler, A., "Catalysis," P. H. Emmett, ed., Vol. 2, Chapt. 2, pp. 105-165, Reinhold, New York (1955).
25. ———, "Advances in Catalysis," Vol. 3, pp 250-326, Academic Press, New York (1951).
26. Yeung, R. S. C., Sc.D. thesis, Mass. Inst. Technol., Cambridge, Massachusetts (1961). See also Satterfield, C. N., and R. S. C. Yeung, *Ind. Eng. Chem. Fundamentals Quart.*, to be published.

Manuscript received October 13, 1961; revision received July 11, 1962; paper accepted July 17, 1962. Paper presented at A.I.Ch.E. Los Angeles meeting.

Dispersed Phase Mixing: I.
Theory and Effects in Simple Reactors

R. L. CURL

Shell Development Company, Emeryville, California

When drops in a two-liquid phase chemical reactor are able to mix with one another by coalescences and redispersions, any spread of concentration among the drops tends to be averaged out. This phenomenon can affect average reaction rate and selectivity in non first-order reactions or mass transfer rate controlled reactions in the dispersed phase. It was found that for mass transfer rate controlled reactions, or the equivalent zero-order reaction, quite large dispersed phase mixing rates are required to bring conversions close to the level obtained with complete mixing.

A well-stirred flow reactor which contains two immiscible liquid phases generally can be treated as an ideal stage with respect to the residence time distribution and the concentration uniformity of the continuous phase. For the dispersed phase however the distribution of concentration among the drop population in the same vessel depends not only upon the residence time distributions and reaction or mass transfer conditions but also upon the number of coalescences and redispersions that occur during a nominal residence time. Therefore when a chemical reaction of other than first order occurs in the dispersed phase in such a reactor, mixing of that phase can have an important effect on the reactor size required for a given conversion or on the conversion and selectivity in a given reactor. The two extremes of no mixing and complete mixing of the dispersed phase have been considered by Rietema (5) for a single-stage reactor in which a zero-order reaction is proceeding in the dispersed phase. He calculated the ratio of residence times required for a given conversion for these two cases and found for example that mixing can make a factor of 3 difference at 80% conversion.

More recently Madden and Damerell (3) have described work in which they measured the rate of dispersed phase mixing in a 5½ in. diameter stirred vessel. The question naturally arises of whether under particular circumstances a certain measured rate of dispersed phase mixing represents a case closer to no mixing or to complete mixing. It would also be desirable to estimate the actual effect of mixing on the conversion or selectivity in a particular system. A mathematical model is presented here for the simultaneous effects of reaction, mass transfer, and dispersed phase mixing in a continuous flow stirred reactor. From this there are obtained the consequences in batch mixing, zero-order chemical reactions, and cases of mass transfer controlled reactions in the dispersed phase. The model used is a simplified one. For example it is assumed that all drops in the system are of equal size and have equal probability of coalescing, and that redispersion occurs immediately after a coalescence to form two equal drops.

It is possible to consider any number of combinations of direction of mass transfer, number and order of reaction, consecutive reactions, and series or other arrangements of stages. However the intent here is primarily to suggest a model for dispersed phase mixing which subsequently can be introduced into various reaction and reactor schemes. The examples and applications given here are both by way of example and to provide quantitative answers for a case of basic interest, the zero-order or mass transfer controlled reaction.

There is similarity between the phenomena associated with incomplete dispersed phase mixing and incomplete homogeneous mixing. In the terminology of Danckwerts (1) the latter is segregated flow and is the cause of changes in overall reaction rate for reactions of other than first order. In the homogeneous case the scale of segregation may have a number of definitions as there are no sharp boundaries between the clumps or streaks of different concentrations. In the present case the phase boundary permits a clearer concept of segregation or concentration distribution.

This idea of homogeneous but segregated flow has been extended by Zwietering (8) to continuous flow sys-

R. L. Curl is with Technische Hogeschool Te Eindhoven, Eindhoven, Holland.